Applied Physics Letters

Experimental observation of the inductive electric field and related plasma nonuniformity in high frequency capacitive discharge

S. K. Ahn and H. Y. Chang

Citation: Appl. Phys. Lett. **93**, 031506 (2008); doi: 10.1063/1.2965118
View online: http://dx.doi.org/10.1063/1.2965118
View Table of Contents: http://apl.aip.org/resource/1/APPLAB/v93/i3
Published by the American Institute of Physics.

Additional information on Appl. Phys. Lett.

Journal Homepage: http://apl.aip.org/
Journal Information: http://apl.aip.org/about/about_the_journal
Top downloads: http://apl.aip.org/features/most_downloaded
Information for Authors: http://apl.aip.org/authors

ADVERTISEMENT

Downloaded 22 Apr 2013 to 143.248.118.122. This article is copyrighted as indicated in the abstract. Reuse of AIP content is subject to the terms at: http://apl.aip.org/about/rights_and_permissions

Experimental observation of the inductive electric field and related plasma nonuniformity in high frequency capacitive discharge

S. K. Ahn[a)] and H. Y. Chang
Low-Temperature Plasma Laboratory, Department of Physics, Korea Advanced Institute of Science and Technology, 373-1 Guseong-dong, Yuseong-gu, Daejeon, 305-701, Republic of Korea

(Received 20 November 2007; accepted 8 July 2008; published online 25 July 2008)

To elucidate plasma nonuniformity in high frequency capacitive discharges, Langmuir probe and B-dot probe measurements were carried out in the radial direction in a cylindrical capacitive discharge driven at 90 MHz with argon pressures of 50 and 400 mTorr. Through the measurements, a significant inductive electric field (i.e., time-varying magnetic field) was observed at the radial edge, and it was found that the inductive electric field creates strong plasma nonuniformity at high pressure operation. The plasma nonuniformity at high pressure operation is physically similar to the *E-H* mode transition typically observed in inductive discharges. This result agrees well with the theories of electromagnetic effects in large area and/or high frequency capacitive discharges.
© *2008 American Institute of Physics*. [DOI: 10.1063/1.2965118]

Capacitive discharges are widely used for etching, deposition, and other surface treatments of materials in the fabrication of microelectronic devices.[1] They are typically operated in the electrostatic regime, for which the excitation wavelength λ is much larger than the electrode size, and the plasma skin depth δ is much larger than the electrode spacing. However, recently, the excitation frequency has been increased considerably, because higher plasma density is expected at higher excitation frequencies[2–7] (a low frequency may be added for independent control of the ion energy[8,9]). Additionally, the electrode size has also been increased to facilitate increased process throughput. Consequently, electromagnetic effects and related plasma non-uniformity issues have taken on greater importance and many related studies have been reported during the past decade.[10–16] From theoretical studies, it was shown that if capacitive discharges are driven at high frequencies and/or have a large electrode size, the inductive electric field (which is typically negligible in low frequency, small area capacitive discharges) becomes significant.[10–14] Additionally, in this case, the capacitive discharges may undergo various phenomena related to the inductive electric field.[12–14] It was also shown that the components of the electric field in large area and/or high frequency capacitive discharges (usual capacitive electric field and the inductive electric field) can be spatially nonuniform.[10,11] Meanwhile, through experimental studies, plasma nonuniformities due to the non-uniform capacitive electric field (standing wave effect) were observed.[15] A shaped electrode was used to suppress the standing wave effect.[16] However, the existence and spatial distribution of the inductive electric field in high frequency capacitive discharges have not yet been observed. Thus, plasma nonuniformities related to the inductive electric field still have ambiguities.

In this study, experimental observations of the inductive electric field (i.e., time-varying magnetic field) in a high frequency (90 MHz) capacitive discharge are reported. It is shown that the inductive electric field leads to strong plasma nonuniformity at high pressure operation and that the plasma nonuniformity at high pressure operation is physically similar to the *E-H* mode transition typically observed in inductive discharges.[17]

The experiment was performed in a capacitive reactor that is driven at 90 MHz frequency in argon gas, as shown in Fig. 1. The reactor is composed of two parallel circular electrodes with equal sizes (14 cm in diameter). The lower electrode is a grounded electrode, while the upper electrode is a powered electrode. Both of the electrodes were separated by 4 cm and were positioned at the center of the discharge chamber. To keep the discharge between the two electrodes, a ceramic confinement ring with a diameter equal to that of the electrode and a height of 1 cm was inserted beneath the powered electrode. The rf power delivered to the plasma during the discharge was estimated using the subtractive method.[18] To calculate the capacitive bulk electric field, the discharge current at a given discharge power was measured using a calibrated current pickup coil that was placed on the powered electrode. In this experiment, the standing wave effect was not significant, because the wavelength in the presence of plasma (λ) was much larger than the electrode size (14 cm in diameter). For all the experimental conditions at 90 MHz, λ ranged from 1.3 to 1.6 m (estimated by using the analytical approximation in Ref. 10 under the assumption of a sheath width ranging from 3 to 5 mm).

For plasma diagnostics, a rf compensated Langmuir probe and a B-dot probe were employed. The Langmuir probe was used to measure the local electron density, and the

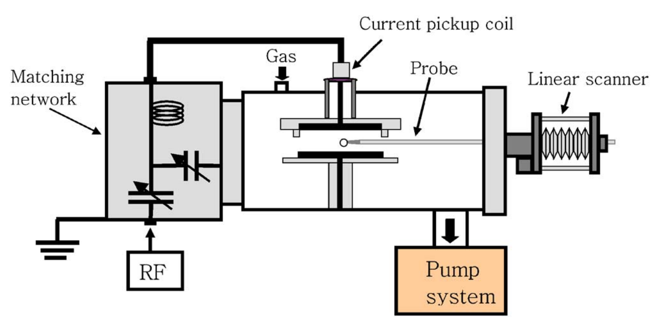

FIG. 1. (Color online) Schematic view of the capacitively coupled plasma chamber.

[a)]Electronic mail: notask@kaist.ac.kr.

Downloaded 22 Apr 2013 to 143.248.118.122. This article is copyrighted as indicated in the abstract. Reuse of AIP content is subject to the terms at: http://apl.aip.org/about/rights_and_permissions

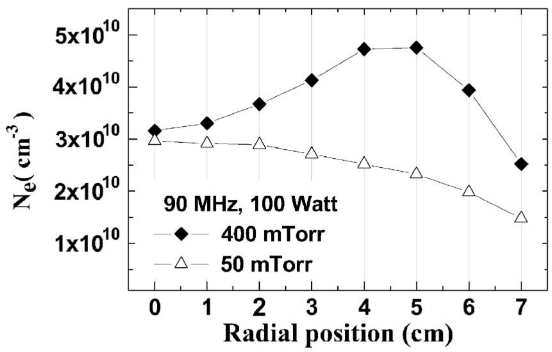

FIG. 2. The electron density as a function of the radial position (0 cm indicates the discharge center) measured at 90 MHz, 100 W, and 50 and 400 mTorr.

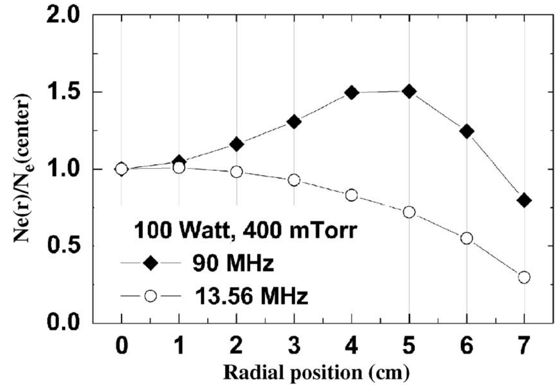

FIG. 3. Comparison of the radial electron density profiles measured at (100 W, 400 mTorr) 13.56 and 90 MHz. For a simple comparison, the electron densities were normalized to the density at the discharge center.

B-dot probe was used to measure the local time-varying magnetic field. Both of the B-dot probe and the Langmuir probe were placed at the center between the two electrodes ($z=2$ cm; henceforth, the surface of the powered electrode is defined as $z=0$) and was driven along the radial direction using a linear scanner. The Langmuir probe system consists of a small probe tip, which was made by a tungsten wire 3 mm long and 0.15 mm in diameter, and a floating reference probe with a resonator-choke coil that reduces the rf distortion of the probe characteristics. In this experiment, the electron density was obtained from measurement of the electron energy distribution function (EEDF).[19,20] The B-dot probe system consists of a single wire loop, which was made by 0.15 mm diameter tungsten wire and has an outer diameter of 6 mm, and a center-tapped transformer that rejects undesired capacitive pickup signals. The normal vector of the probe loop surface was set-parallel to the electrodes in order to measure the time-varying azimuthal magnetic field. The B-dot probe system was calibrated using a rf magnetic field of a known magnitude that was produced by a Helmholtz coil arrangement.[21] The insensitivity of the B-dot probe to capacitive coupling was confirmed by rotating the probe loop surface by 180°.

Figure 2 shows the electron density as a function of the radial position (r; $r=0$ cm indicates the discharge center) measured at 90 MHz, 100 W, and 50 and 400 mTorr. At 50 mTorr, the electron density shows a maximum at the discharge center and gradually decreases along the radial direction. In contrast, at 400 mTorr, the electron density near the radial edge ($r=7$ cm) is much higher compared to that in the discharge center. The electron density profile at 50 mTorr is considered to be a result of radial plasma diffusion. In this experiment, the plasma was not completely confined between the powered and grounded electrode, although the reactor was equipped with a 1 cm high confinement ring beneath the powered electrode (the gap length between the two electrodes was 4 cm). Thus, significant radial plasma diffusion was expected, and this radial plasma diffusion can lead to an electron density profile that is radially decreased. Here, as we previously mentioned, the standing wave effect was not significant. Consequently, the electron density profile at 50 mTorr appears not to have resulted from the standing wave effect.

The electron density profile at 400 mTorr (a much higher electron density near the radial edge) cannot be explained by simple radial diffusion. In addition, this profile did not arise at 13.56 MHz operation with the same discharge power and pressure, as shown in Fig. 3. Thus, the high electron density near the radial edge also cannot be explained by the usual electrostatic interpretations. In order to understand the result, the inductive electric field (i.e., the time-varying magnetic field) was investigated on the basis of B-dot probe measurement. Figure 4 shows the amplitude of the azimuthal magnetic field and corresponding inductive electric field as a function of the radial position under discharge conditions identical to those in Fig. 2. The inductive electric field was calculated from the measured azimuthal magnetic field by applying the integral form of Faraday's law to the probe loop.

To compare the amplitude of the inductive electric field with that of the capacitive bulk electric field, the capacitive bulk electric field was calculated using the measured discharge current (I_D). As noted previously, a calibrated current pickup coil was used to measure the discharge current. In the bulk plasma, assuming that the discharge current flow is almost completely due to the electron conduction, the discharge current density (J_D) can be expressed as follows:

$$J_D \approx J_e = en_e u_e = e^2 n_e \frac{E_b}{m_e\sqrt{\omega^2+\nu_m^2}}, \tag{1}$$

where J_e, n_e, u_e, m_e, ω, and ν_m are the electron conduction current density in the bulk plasma, the electron density, the electron drift velocity, the electron mass, the angular rf frequency, and the momentum transfer collision frequency (calculated from the measured EEDF), respectively. The amplitude of the capacitive bulk electric field at the discharge

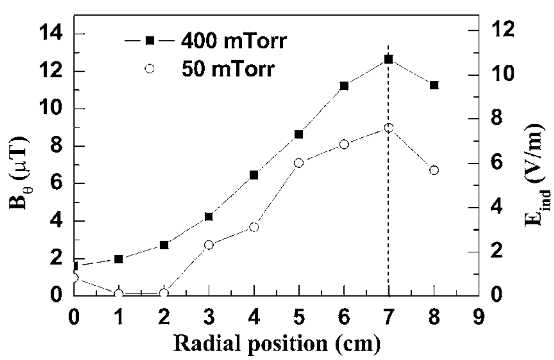

FIG. 4. Amplitude of the azimuthal magnetic field (B_θ) and corresponding inductive electric field (E_{ind}) as a function of the radial position at 90 MHz, 100 W, and 50 and 400 mTorr.

Downloaded 22 Apr 2013 to 143.248.118.122. This article is copyrighted as indicated in the abstract. Reuse of AIP content is subject to the terms at: http://apl.aip.org/about/rights_and_permissions

center was calculated using Eq. (1). From the calculation, the amplitudes of the capacitive bulk electric field at the discharge center were found to be 66.52 V/m at 50 mTorr (J_D=10.05 mA/cm^2) and 113.99 V/m at 400 mTorr (J_D=12.18 mA/cm^2).

As shown in Fig. 4, the amplitude of the inductive electric field at the radial center is very small compared to those for the capacitive bulk electric field. However, the values at the radial edge (r=7 cm) amount to 10% of the capacitive bulk electric field. Moreover, considering that the probe measurements were performed at the axial center between the two electrodes (z=2 cm) and that the inductive electric field rapidly decays within the bulk plasma,[22,23] a much stronger inductive electric field is expected near the plasma-sheath boundary below the radial edge of the powered electrode. For example, in the case of using the data in Ref. 23 and assuming a sheath width of 3 mm, the inductive electric field at this region ($z\sim 0.3$ cm and r=7 cm) can be estimated as about 50 V/m (about 44% of the capacitive bulk electric field) at 400 mTorr.

Depending on the pressure, the inductive electric field largely localized near the radial edge can affect the radial plasma uniformity in different manners. At high pressures where the electron energy relaxation length (λ_ε) is much smaller than the discharge radius ($\lambda_\varepsilon \approx \sqrt{\lambda\lambda^*}$, where λ and λ^* are the electron mean free paths for the elastic and inelastic collisions, respectively), the electron density becomes a nearly local function of the electric field intensity. Thus, at the radial edge where the net rf electric field intensity in the bulk plasma (E_b+E_{ind}) is much stronger compared to that at the radial center, much higher electron density is expected. The radial electron density profile at 400 mTorr (-◆- in Fig. 2) can be understood in this manner. However, at low pressures where λ_ε exceeds the discharge radius, the electron density is not a local function of the electric field but a function of the spatially averaged electric field. Thus, at 50 mTorr, although a significant inductive electric field exists at the radial edge, corresponding nonuniformity of the radial electron density cannot be observed, as shown in Fig. 2 (-△-).

On the other hand, at 400 mTorr, the electrons at the radial center are mostly heated by the capacitive electric field (E_{ind} is very small at the radial center); consequently, the discharge at the radial center can be interpreted as a pure capacitive discharge. However, near the radial edge, the electrons are heated by both the capacitive electric field and the inductive electric field localized at this region; consequently, the discharge near the radial edge experiences significant inductive coupling. The change in electron heating along the radial direction is similar to the change in electron heating during the E-H mode transition in inductive discharges.[17] This result is in good agreement with theoretical predictions (the spatial E-H mode transition in high frequency capacitive discharges),[13,14] and it is believed that much clearer spatial E-H mode transitions will be observed if the discharge is operated using much larger electrodes and/or higher excitation frequencies.

In conclusion, through Langmuir probe and B-dot probe measurements in a cylindrical high frequency capacitive discharge, it was found that there is a significant inductive electric field (i.e., time-varying magnetic field) near the radial edge, and the inductive electric field creates strong plasma nonuniformity at high pressure operation (a much higher electron density near the radial edge).

The authors are grateful to Dr. S. J. You and Dr. S. W. Lee for their helpful comments on this work. This work was sponsored in part by the Tera Level Nanodevices Project of MOST (TND, Grant No. M103KC010006-07K0301-00620). It was also supported in part by Grant No. R11-2000-086-0000-0 from the Center of Excellency Program of KOSEF, MOST, and the Korea Ministry of Education through the Brain Korea 21 Program.

[1]B. Chapman, *Glow Discharge Processes* (Wiley, New York, 1980).
[2]M. Surendra and D. B. Graves, Appl. Phys. Lett. **59**, 2091 (1991).
[3]V. Vahedi, C. K. Birdsall, M. A. Lieberman, G. DiPeso, and T. D. Rognlien, Phys. Fluids B **5**, 2719 (1993).
[4]M. J. Colgan, M. Meyyappan, and D. E. Murnick, Plasma Sources Sci. Technol. **3**, 181 (1994).
[5]T. Kitajima, Y. Takeo, N. Nakano, and T. Makabe, J. Appl. Phys. **84**, 5928 (1998).
[6]E. Abdel-Fattah and H. Sugai, Appl. Phys. Lett. **83**, 1533 (2003).
[7]E. Amanatides and D. Mataras, J. Appl. Phys. **89**, 1556 (2001).
[8]P. C. Boyle, A. R. Ellingboe, and M. M. Turner, J. Phys. D **37**, 697 (2004).
[9]H. C. Kim and J. K. Lee, Phys. Rev. Lett. **93**, 085003 (2004).
[10]M. A. Liebermann, J. P. Booth, P. Chabert, J. M. Rax, and M. M. Turner, Plasma Sources Sci. Technol. **11**, 283 (2002).
[11]P. Chabert, J. L. Raimbault, J. M. Rax, and M. A. Lieberman, Phys. Plasmas **11**, 1775 (2004).
[12]P. Chabert, J. L. Raimbault, P. Levif, J. M. Rax, and M. A. Lieberman, Phys. Rev. Lett. **95**, 205001 (2005).
[13]P. Chabert, J. L. Raimbault, P. Levif, J. M. Rax, and M. A. Lieberman, Plasma Sources Sci. Technol. **15**, s130 (2006).
[14]P. Chabert, J. Phys. D **40**, R63 (2007).
[15]A. Perret, P. Chabert, J. P. Booth, J. Jolly, J. Guillon, and Ph. Auvray, Appl. Phys. Lett. **83**, 243 (2003).
[16]H. Schmidt, L. Sansonnens, A. A. Howling, Ch. Hollenstein, M. Elyaakoubi, and J. P. Schmitt, J. Appl. Phys. **95**, 4559 (2004).
[17]U. Kortshagen, N. D. Gibson, and J. E. Lawler, J. Phys. D **29**, 1224 (1996).
[18]V. A. Godyak and R. B. Piejak, J. Vac. Sci. Technol. A **8**, 3833 (1990).
[19]M. A. Lieberman and A. J. Lichtenberg, *Principles of Plasma Discharges and Materials Processing* (Wiley, New York, 1994).
[20]V. A. Godyak, R. B. Piejak, and B. M. Alexandrovich, Plasma Sources Sci. Technol. **1**, 36 (1992).
[21]C. M. Franck, O. Grulke, and T. Klinger, Rev. Sci. Instrum. **73**, 3768 (2002).
[22]R. Piejak, V. A. Godyak, and B. Alexandrovich, J. Appl. Phys. **81**, 3416 (1997).
[23]R. Piejak, V. A. Godyak, and B. Alexandrovich, J. Appl. Phys. **78**, 5296 (1995).

Downloaded 22 Apr 2013 to 143.248.118.122. This article is copyrighted as indicated in the abstract. Reuse of AIP content is subject to the terms at: http://apl.aip.org/about/rights_and_permissions